CHEMPHYSCHEM

DOI: 10.1002/cphc.201000004

Electronic Properties of Propylamine-Functionalized Single-Walled Carbon Nanotubes

Matthias Müller,*[a] Reinhard Meinke,[a] Janina Maultzsch,[a] Zois Syrgiannis,[b] Frank Hauke,[b] Áron Pekker,[c] Katalin Kamarás,[c] Andreas Hirsch,[d] and Christian Thomsen[a]

We present resonant Raman measurements on single-walled carbon nanotubes (SWCNT) functionalized with propylamine groups at different degrees. Direct nucleophilic addition based on in situ generated primary amides is used for attaching *n*-propylamine to the sidewalls of SWCNTs. The influence of the amino functionalities on the electronic structure of the nanotubes is investigated. From the Raman resonance profiles of the radial breathing modes (RBMs), the chiral indices of the corresponding tubes are assigned. We observe significant redshifts of the transition energies and a broadening of the resonance windows due to chemical modification of SWCNTs. Similar redshifts are derived from the analysis of the NIR/Vis transmission spectrum. The relative Raman intensities of the functionalized samples and the evaluation of their transmission spectra indicate a diameter dependence of the reactivity as it has been observed for other moieties. By analyzing the defect induced D mode we observe a considerable degree of functionalization accompanied by an almost unharmed tube structure, which ensures that the observed effects are mainly driven by changes of the electronic structure.

1. Introduction

Covalent sidewall functionalization of carbon nanotubes has become a key issue for a variety of nanotube applications and therefore the chemical reactions have been reviewed in many related articles.[1,2] To attack the tubes framework, quite harsh reaction conditions are necessary to overcome the problem of low inherent reactivity of the tube.[3] A major task of synthesis and characterization is the improvement of the solubility of carbon nanotubes in certain media.

The understanding of how a functional group influences the atomic structure of the tube and its electronic structure is an important topic in view of possible applications. Raman spectroscopy and transmission spectroscopy are powerful non-destructive techniques for the investigation of both structural changes in the tube lattice and changes of the electronic structure of nanotubes.[4] The electronic structure and therefore the tube species are supposed to play a major role in the selectivity of the chemical reaction. It is among the most desirable achievements of carbon nanotube chemistry to overcome the non-selectivity of the growth process. Higher reactivity of metallic tubes has been reported for various moieties,[5,6] and can be explained by several theories.[7,8] The reactivity is also dependent on the diameter of the nanotubes due to curvature effects.[9,10] It is well-known that the optical transitions are highly sensitive to the tube environment, solvents, bundling, doping etc.[11–13] Therefore, analyzing the influence of chemical modification one has always to take into account a possible overlap of these effects. Structural changes such as defects in the nanotube also lead to changes in spectroscopic features.[14]

Here we report the effect of *n*-propylamine functionalization on the optical transitions of single-walled carbon nanotubes. The reaction used here is a two-step process: a direct nucleophilic addition followed by reoxidation in oxygen of a negatively charged (*n*PrNH)*n*-SWCNT^{n-} intermediate that leads to covalently bound amine functionalities as shown in Figure 1).[15,16] This reaction causes a drastic increase of the solubility of the SWCNT-derivative in organic solvents. Therefore a functionalization sequence based on amines provides a promising tool towards SWCNT derivatives with a rich variety of functional groups.

We observe shifts in the transition energies and a broadening of the resonance profiles. The change of the tube environment leads to variations in the intensity of the radial breathing mode (RBM) showing the influence on the electronic structure. Investigation of the defect-induced *D* mode and high energy mode (HEM) after annealing indicates a highly efficient and well-controllable reaction that fulfills the requirement to preserve the intact tube structure, such that the sidegroups can be eliminated completely, leaving both the sigma- and pi-system intact. Therefore influences on the optical transitions due to structural effects can be ruled out.

[a] *M. Müller, R. Meinke, Prof. Dr. J. Maultzsch, Prof. Dr. C. Thomsen*
Institut für Festkörperphysik
Technische Universität Berlin, Hardenbergstr. 36, 10623 Berlin (Germany)
Fax: (+49) 30 314 27705
E-mail: mueller@physik.tu-berlin.de

[b] *Z. Syrgiannis, Dr. F. Hauke*
Zentralinstitut für Neue Materialien und Prozesstechnik
Universität Erlangen-Nürnberg, Dr.-Mack-Str. 81, 90762 Fürth (Germany)

[c] *Á. Pekker, Prof. Dr. K. Kamarás*
Research Institute for Solid State Physics and Optics
Hungarian Academy of Sciences, P.O. Box 49, H-1525 Budapest (Hungary)

[d] *Prof. Dr. A. Hirsch*
Department of Chemistry and Pharmacy
Universität Erlangen-Nürnberg, Henkestr. 42, 91054 Erlangen (Germany)

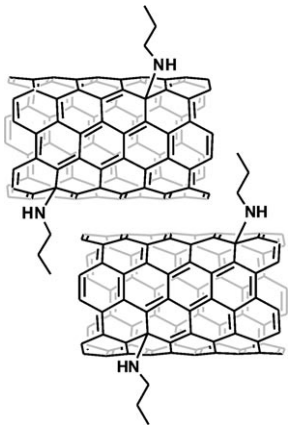

Figure 1. Sketch of a carbon nanotube structure functionalized with propylamine groups.

Experimental Methods

SWNTs were obtained from Carbon Nanotechnologies Inc. (Purified HiPCo© Single-Wall Carbon Nanotubes, Lot number: B0335) and used without further purification or treatment. Chemicals and solvents were purchased from Acros (Geel, Belgium) and used as received.

The solution of lithium amide was prepared as follows: In a nitrogen-purged and heat dried four-necked round bottom flask (250 mL), equipped with two gas inlets and pressure compensation, *n*-propyl amine (f1 = 0.5 mmol, f4 = 10.0 mmol) was dissolved in dry THF. The solution was cooled to 0 °C for 15 min. To this solution the respective amount of *n*-butyllithium (90% of the *n*-propyl amine amount) was added dropwise over a period of 10 min. Then the solution was stirred at room temperature for 1 h. In another 250 mL nitrogen-purged and heat dried three-necked round bottom flask, equipped with two gas inlets, 5 mg of purified HiPCo SWCNTs were dispersed in 100 mL anhydrous solvent (THF) by sonication (15 min). This dispersion of SWCNTs was added to the first flask through a heat dried dropping funnel. After the completion of the addition, the resulting suspension was stirred for 30 min at room temperature and sonicated for 30 min, resulting in a stable, black, homogeneous dispersion. The reaction mixture was stirred at room temperature overnight and subsequently quenched by bubbling oxygen for 1 h through the solution. The resulting dispersion was diluted with 100 mL cyclohexane, transferred to a separation funnel and purged with water. The organic layer with the nanotubes was filtered through a 0.2 mm PP membrane filter and washed with cyclohexane, methanol, ethanol and water. The resulting black solid was dried in a vacuum oven at 50 °C overnight.

The resonant Raman measurements were carried out using a micro-Raman setup in backscattering geometry, the samples being excited by a tunable laser with about 0.4 mW laser power on the samples. A charge-coupled device is used to detect the signal after analyzing the signal via a triple monochromator. We recorded spectra of samples functionalized to different degrees, 2% (f1) and 6% (f4) respectively, and spectra of the non-functionalized starting material for comparison. The spectrometer was calibrated in frequency using a Neon lamp. Bulk CaF_2 was used to normalize the intensities of the RBM signal at different excitation energies.

For wide range transmission spectroscopy, transparent self supporting films were prepared by filtration.[17,18] Transmission spectra were taken by Bruker IFS66v (far-, mid-infrared), Bruker Tensor 27 (mid-, near infrared) Fourier transformation spectrometers and a Jasco V550 (visible, ultraviolet) spectrophotometer. For further analysis the optical conductivity was calculated using the Kramers-Kronig method and model considerations (Optical conductivity in a solid sample scales more accurately with charge concentration than the optical density $-\log T$.).[19] For these calculations the thickness of the samples was measured by atomic force microscopy.

2. Results

2.1. RBM and Optical Transitions

Full resonance profiles for the second transition of semiconducting tubes E_{22}^S and the first transition of metallic tubes E_{11}^M have been recorded, the chiral indices were assigned following the procedure of refs. [11, 20]. Due to bundling the transition energy of all our samples including the starting material is redshifted in comparison to the data taken on dissolved nanotubes in the related articles. Figure 2a shows the resonance

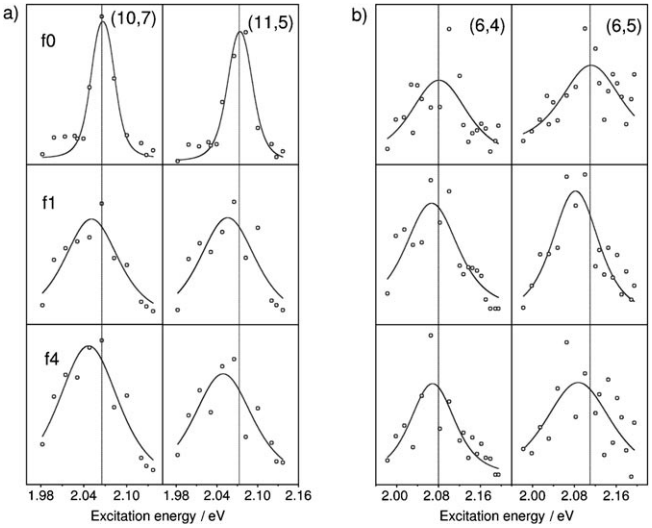

Figure 2. Resonance profiles: reference samples (top), functionalized samples with 2% (middle, f1) and 6% (bottom, f4) degree of functionalization. a) metallic tubes b) semiconducting tubes. The profiles are fitted according to ref. [11].

profiles of tubes belonging to the E_{11}-transition of the metallic (13,1) branch. Both functionalized samples show a pronounced redshift of the optical transition accompanied by a broadening of the resonance window compared to the reference sample. Comparable effects are also observed for the E_{22} of semiconducting tubes as shown in Figure 2b. The average transition energy shift between the non-functionalized material and the functionalized samples is about 20 meV to lower energies for the lower degree of functionalization (f1) and about 25 meV for the higher one (f4) (see also Table 1). This is consistent with our findings concerning the tube reactivity: all our data, including UV/Vis/NIR absorption show a redshift of the optical

Table 1. Transition energies obtained from Raman resonance profiles for various metallic and semiconducting nanotubes, *g*: fit parameter related to the width of the resonance window from ref. [11]. f0: pristine tubes, f1/f4: lower/higher functionalized sample.

(*n*,*m*)	Sample	E_{ii} [eV]	γ
(6,4)	f0	2.072	0.100
	f1	2.046	0.167
	f4	2.048	0.143
(6,5)	f0	2.084	0.116
	f1	2.063	0.151
	f4	2.068	0.222
(10,7)	f0	2.054	0.040
	f1	2.038	0.133
	f4	2.034	0.150
(13,1)	f0	2.053	0.035
	f1	2.022	0.118
	f4	2.031	0.114
(11,5)	f0	2.061	0.050
	f1	2.043	0.146
	f4	2.036	0.154
(12,3)	f0	2.057	0.066
	f1	2.024	0.155
	f4	2.020	0.185

transition but do not indicate a selectivity between metallic and semiconducting nanotubes towards the direct nucleophilic addition.[15]

Wide range transmission spectroscopy and Raman spectroscopy are complementary methods. By utilizing the benefits of both techniques we can make our results more reliable. Transmission spectroscopy provides information about the electronic structure of the nanotubes. The absence of resonance conditions makes this method suitable for measuring all nanotube species in the sample, but lacks the possibility to assign these features to specific tubes. Changes in the electronic structure have direct influence on the features of the optical spectrum. By investigating the spectra of samples functionalized to different degrees, we observe shifts in the transition energies and a frequency dependent decrease of transition intensities. The Raman resonance profiles follow the absorption spectrum of a specific type of nanotube, transmission spectra on the other hand yield the overall spectrum of the nanotube ensemble. It should be noted that the absolute values for the transition energies obtained from the different spectroscopic methods cannot be compared, because the samples have been prepared either in solution or as bulk material. It is well-known that these different environments lead to shifts of the optical transitions.[13] NIR/VIS optical conductivity spectra were fitted by Lorentzians. To reduce the fitting error of peak position determination, the fitted peaks were subtracted from the measured spectrum except the peak of our concern. This residual spectrum contains only one peak and its position can be defined using standard methods. Comparison of the peak positions of different samples results in most of the peaks being redshifted as a consequence of functionalization (Figure 3). Although these shifts have the same trends as in the case of Raman measurements, the magnitudes are considerably smaller. The possible explanation is that without resonance condition we measure the contribution of all nanotubes at certain energies. These overlapping peaks, especially the ones related to the unaffected tubes, make the shifts less pronounced. To investigate the effect of functionalization on the whole nanotube mixture, the group of E_{11}^S and E_{22}^S peaks of different samples was compared. The evolution of the intensities of the first and second semiconducting transitions indicates the diameter selectivity of the functionalization. The higher frequency part of the peaks is related to nanotubes with smaller diameter. In Figure 4 the high frequency part of both the first and second transition peaks decrease in the case of functionalized samples. This proves the higher reactivity of smaller tubes.

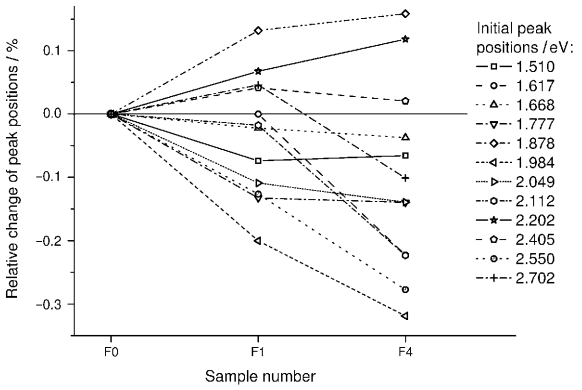

Figure 3. The evolution of the peak positions related to E_{22}^S transitions from optical conductivity measurements. The plot shows the relative change in the position of the different E_{22}^S peaks versus the sample type [from left to right: pristine tube (f0), lower/higher (f1,f4) functionalized sample].

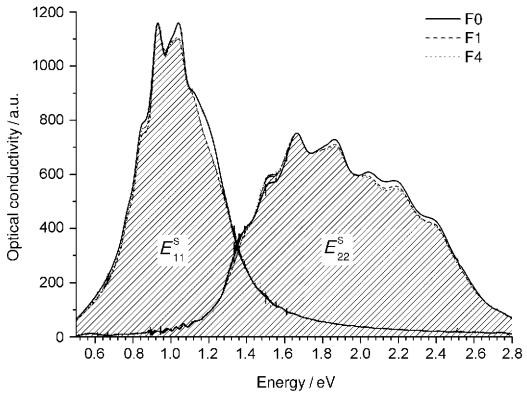

Figure 4. The effect of functionalization on the E_{11}^S and E_{22}^S transitions. The higher frequency part of the peaks decrease due to higher reactivity of the smaller diameter tubes. The area under the peaks related to the higher functionalized sample was striped to emphasize the change in the intensity.

The effect on the optical transition can be explained by a charge transfer between the tube and the functional group. The charge transfer arises from the attachment of a heteroatom (nitrogen) to the sidewall of the tube due to the difference in electronegativity. The polar bonding appears as a doping effect, introducing donor or acceptor levels within the gap of the E_{ii} transition. This leads to a redshift, because the ef-

fective gap is decreased, and in a broadening of the resonance window, because it offers more real states to be possibly matched in an incoming or outgoing resonance of the Raman process. In this picture the shifts are completely independent of the reaction sequence itself. This is consistent with recent results on nanotubes functionalized with Ru^{II}-terpyridine complexes which also show a redshift.[21,22] Additionally, in previous work on non-polar covalent bonding such as alkyl chains, no comparable shifts of the transition energy have been observed.[23] For larger charge transfer the displacement of the Fermi level itself and its movement towards either valence or conduction band has to be taken into account, which leads to an increase in the difference of electronic states between conduction band and occupied valence band, inducing a blueshift. Therefore the amount of charge transfer due to functionalization is determined by the degree of functionalization as well as the polarity of the bond. Fantini et al. have studied similar effects on SWCNTs functionalized with diazonium salts.[24] Their *D*/*G* ratio is larger than one[24] though the degrees of functionalization are smaller than in our case. This larger *D*/*G* ratio may indicate also structural changes in addition to the "defects" introduced by the covalent bonds. However they show a similar behavior to our results concerning energy shifts.

The decrease of the RBM intensities due to functionalization is commonly used to investigate the reactivity depending on either tube species or diameter. For this purpose it is of particular importance to analyze the influence of functionalization on the resonance condition. This ensures that the changes in intensity refer to the quenching due to loss of translational symmetry and are not merely due to leaving the resonance window. The predominant effect determining the chemical reactivity in our samples is the tube diameter as it has been reported for other reactions.[21,23] This curvature effect, shown above for the optical transitions, can easily be seen from Figure 5. The RBM intensity is attenuated on functionalization; this becomes more and more pronounced for small diameters, that is at higher Raman shifts. We observe this by normalizing to certain tube chiralities. A comparison of the absolute values of the Raman intensities between different samples is not possible, because due to the preparation process the surface of the bulk material is changed. Therefore, we obtained very different absolute intensities for the functionalized samples. The curvature effect arises because of different pyramidalization and *p*-orbital misalignment angles in carbon nanotubes of different diameter. Local strain for tubes of smaller diameter can be partially relaxed by sidewall addition.[9] This concept also reveals the different chemistry of fullerenes and nanotubes.[10] Concerning the Raman frequencies of the RBMs, only slight shifts are observable. All RBMs are shifted within our experimental error of about 1 cm^{-1}, but show a clear trend to higher frequencies. It should be noted that the width and lineshape of the RBMs seem unaffected.

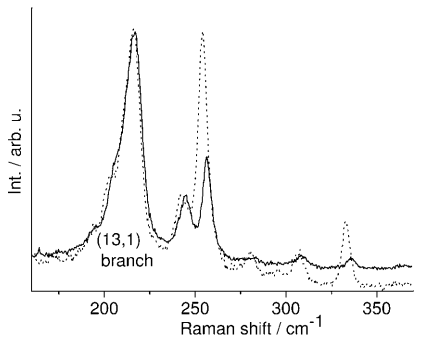

Figure 5. Raman spectra taken in resonance of the (13,1) tube of pristine (f0, excitation energy: 2.05 eV) and functionalized material (f4, 2.03 eV) respectively, probing various nanotubes. The intensities are normalized to the RBM of the (13,1) tube. (——): functionalized sample, (– – –): starting material.

2.2. HEM and D Mode Features

The *D* mode at about 1320 cm^{-1} arises from a double-resonant scattering process which reveals structural changes in the tube framework.[25,26] Its intensity is a measure of quality or homogeneity of a sample. Traditionally its intensity is normalized to the Raman-allowed *G*-peak, although normalization to the second-order *D** peak would be more appropriate for quantitative evaluation.[27] For inspection of the sample quality, however, the *D*/*G* ratio is adequate and shown in Figure 6 for the functionalized sample f4. In the case of functionalized tubes the *D* mode may reflect both a successful addition reaction or a possible damage of the tube during the reaction. The intensity of this mode increases with the concentration of defects in a nanotube.[14] The successful sidewall addition similarly breaks the translational symmetry and changes the Raman selection rules resulting in an increased *D* mode intensity.[6,28] From another point of view the covalent bonds change the hybridization of the attacked carbon atoms from sp^2 to sp^3 and therefore make a contribution to the *D* mode intensity. Figure 7 shows Raman spectra of the functionalized sample f4 before and after annealing together with the starting material. The *D* mode intensity increases on functionalization. After annealing, the intensity is even weaker than in the pristine material. This clearly shows that the side groups can be eliminated leaving the sigma-bonds intact and the pi-system reconstructed. This is important to ensure that the observed changes in the transition energies are predominantly driven by charge transfer and less related to structural damage of the tube.

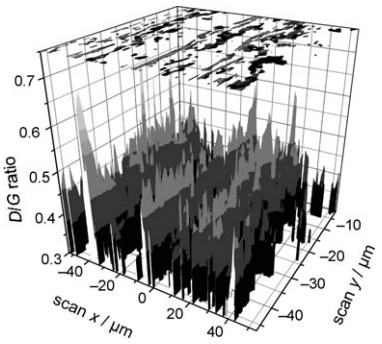

Figure 6. Normalized *D*/*G* ratio mapping of sample f4.

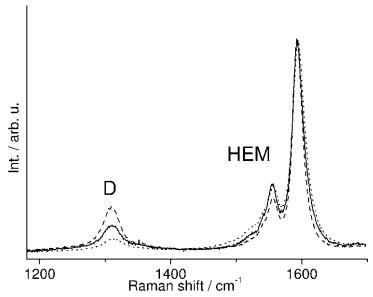

Figure 7. *D* mode and HEM of functionalized sample f4 (– – –), annealed (•••••) and reference samples (——) at 633 nm excitation wavelength. The HEM in the three spectra are very similar, indicating that there are no significant doping effects.

Concerning the high energy modes (HEM) of either functionalized and reference samples, no significant shifts with functionalization are observable; the lineshape is also unaffected. Only a slight decrease of the G^- peak can be seen. After annealing, the intensity of the G^- peak is restored. The absence of hardening or softening of the HEM indicates a quite low doping level as compared to, e.g., electrochemical doping.[29] This supports our findings concerning the redshift of the optical transitions as described above.

3. Conclusions

We have shown by optical spectroscopic methods how functional groups affect the electronic properties of carbon nanotubes. For the applied reaction, a direct nucleophilic addition based on in situ generated primary amides, we observe a significant redshift of the optical transitions together with a broadening of the resonance window. We relate this behavior to the polar nature of the bond between the nanotube and the amine group. The Raman spectra indicate a pronounced diameter dependence of the chemical reaction. Furthermore, the Raman spectra confirm that the chemical reaction does not disturb the atomic structure of the nanotube itself. Therefore, the observed effects on the optical transitions are mainly due to charge transfer. Further studies on the influence of different degree of functionalization and bond polarity, that is, different moieties, seem promising.

Acknowledgement

A.H. thanks the Deutsche Forschungsgemeinschaft and the Interdisciplinary Center for Molecular Materials for financial support. The Berlin authors acknowledge support by the cluster of excellence "UniCat", funded by the DFG. Work in Hungary was supported by the Hungarian Scientific Research Fund OTKA under grant No. T075813 and European Commission NMP4-CT-2006-031847 NEURONANO.

Keywords: carbon · electronic structure · nanotubes · Raman spectroscopy

[1] P. Singh, S. Campidelli, D. Bonifazi, A. Bianco, M. Prato, *Chem. Soc. Rev.* **2009**, *38*, 2214.
[2] A. Hirsch, O. Vostrowsky, *Functionalization of Carbon Nanotubes*, Wiley-VCH, Weinheim, **2007**.
[3] A. Hirsch, O. Vostrowsky, *Top. Curr. Chem.* **2005**, *245*, 193.
[4] S. Reich, C. Thomsen, J. Maultzsch, *Carbon Nanotubes*, Wiley-VCH, Weinheim, **2004**.
[5] H. Hu, B. Zhao, M. A. Hamon, K. Kamaras, M. E. Itkis, R. C. Haddon, *J. Am. Chem. Soc.* **2003**, *125*, 14893.
[6] R. Graupner, J. Abraham, D. Wunderlich, A. Vecelová, P. Lauffer, J. Rörl, M. Hundhausen, L. Ley, A. Hirsch, *J. Am. Chem. Soc.* **2006**, *128*, 6683.
[7] M. S. Strano, C. A. Dyke, M. L. Usrey, P. W. Barone, M. J. Allen, H. Shan, C. Kittrell, R. H. Hauge, J. M. Tour, R. E. Smalley, *Science* **2003**, *301*, 1519.
[8] E. Joselevich, *ChemPhysChem* **2004**, *5*, 619.
[9] Z. Chen, W. Thiel, A. Hirsch, *ChemPhysChem* **2003**, *4*, 93.
[10] S. Niyogi, M. A. Hamon, H. Hu, B. Zhao, P. Bhowmik, R. Sen, M. E. Itkis, R. C. Haddon, *Acc. Chem. Res.* **2002**, *35*, 1105.
[11] J. Maultzsch, H. Telg, S. Reich, C. Thomsen, *Phys. Rev. B* **2005**, *72*, 205438.
[12] M. J. O'Connell, S. Sivaram, S. K. Doorn, *Phys. Rev. B* **2004**, *69*, 235415.
[13] O. Kiowski, S. Lebedkin, F. Hennrich, S. Malik, H. Rösner, K. Arnold, C. Sürgers, M. M. Kappes, *Phys. Rev. B* **2007**, *75*, 075421.
[14] V. Skákalová, J. Maultzsch, Z. Osváth, L. P. Biró, S. Roth, *Phys. Status Solidi RRL* **2007**, *1*, 138.
[15] Z. Syrgiannis, F. Hauke, J. Röhrl, M. Hundhausen, R. Graupner, Y. Elemes, A. Hirsch, *Eur. J. Org. Chem.* **2008**, 2544.
[16] Z. Syrgiannis, B. Gebhardt, C. Dotzer, F. Hauke, R. Graupner, A. Hirsch, *Angew. Chem.* **2010**, *122*, 3394; *Angew. Chem. Int. Ed.* **2010**, *49*, 3322.
[17] F. Hennrich, R. Wellmann, S. Malik, S. Lebedkin, M. M. Kappes, *Phys. Chem. Chem. Phys.* **2003**, *5*, 178.
[18] Z. Wu, Z. Chen, X. Du, J. Logan, J. Sippel, M. Nikolou, K. Kamarás, J. R. Reynolds, D. B. Tanner, A. F. Hebard, A. G. Rinzler, *Science* **2004**, *305*, 1273.
[19] Á. Pekker, F. Borondics, K. Kamarás, A. G. Rinzler, D. B. Tanner, *Phys. Status Solidi B* **2006**, *243*, 3485.
[20] H. Telg, J. Maultzsch, S. Reich, F. Hennrich, C. Thomsen, *Phys. Rev. Lett.* **2004**, *93*, 177401.
[21] M. Müller, J. Maultzsch, K. Papagelis, A. A. Stefopoulos, E. K. Pefkianakis, A. K. Andreopoulou, J. K. Kallitsis, C. Thomsen, *Phys. Status Solidi B* **2009**, *246*, 2721.
[22] A. A. Stefopoulos, E. K. Pefkianakis, K. Papagelis, A. K. Andreopoulou, J. K. Kallitsis, *J. Polym. Sci. Part A* **2009**, *47*, 2551.
[23] M. Müller, J. Maultzsch, D. Wunderlich, A. Hirsch, C. Thomsen, *Phys. Status Solidi B* **2008**, *245*, 1957.
[24] C. Fantini, M. L. Usrey, M. S. Strano, *J. Phys. Chem. C* **2007**, *111*, 17941.
[25] J. Maultzsch, S. Reich, C. Thomsen, *Phys. Rev. B* **2001**, *64*, 121407.
[26] C. Thomsen, S. Reich, *Phys. Rev. Lett.* **2000**, *85*, 5214.
[27] J. Maultzsch, H. Telg, S. Reich, C. Thomsen, *Phys. Rev. B* **2004**, *70*, 155403.
[28] M. Müller, J. Maultzsch, D. Wunderlich, A. Hirsch, C. Thomsen, *Phys. Status Solidi RRL* **2007**, *1*, 144.
[29] P. M. Rafailov, J. Maultzsch, C. Thomsen, *Phys. Rev. B* **2005**, *72*, 045411.

Received: January 5, 2010
Published online on June 29, 2010

